

Supplementary Materials for **Canopy near-infrared reflectance and terrestrial photosynthesis**

Grayson Badgley, Christopher B. Field, Joseph A. Berry

Published 22 March 2017, *Sci. Adv.* **3**, e1602244 (2017)

DOI: 10.1126/sciadv.1602244

This PDF file includes:

- text S1. Sellers' two-stream approximation
- text S2. 2D reflectance model
- text S3. NIR_v and SIF simulations using SCOPE
- table S1. Parameter values for two-stream approximation model.
- table S2. Model parameters used in 2D reflectance model.
- table S3. Parameter ranges used in 2D reflectance model sensitivity test.
- table S4. SCOPE parameter values.
- table S5. Multiyear monthly average NIR_v, fPAR, and GPP, by land cover classification for 105 FLUXNET sites.
- fig. S1. NIR_v more strongly predicts canopy fPAR than does NDVI.
- fig. S2. NIR_v as a function of NDVI and NIR_T.
- fig. S3. Linear relationship between modeled NIR_v and SIF.
- fig. S4. Comparison of the monthly MODIS-derived (A) NIR_T and (B) NIR_v against GOME-2 measurements of SIF.
- References (37, 38)

text S1. Sellers' two-stream approximation

Here we demonstrate that multiplying NIR_T by NDVI better approximates canopy fPAR, using a two-stream radiative transport model fully described in (8–10). Calculating reflectances requires specifying a leaf angle distribution, the total leaf area, soil reflectance, and a wavelength-dependent scattering coefficient. A full list of parameters and their ranges is presented in table S1. We assumed a spherical leaf angle distribution for all simulations.

table S1. Parameter values for two-stream approximation model.

Parameter	Values
Visible scattering coefficient (ω_V)	0.2
Near-infrared scattering coefficient (ω_N)	0.95
Soil reflectance (ρ_S)	0.05 - 0.5
Leaf area (L_T)	0 - 8

We calculated reflectance in the visible (R_T) and in the near-infrared (N_T) part of the spectrum. From the resulting reflectance data, we calculated NDVI and NIR_V , where NDVI equals

$$NDVI = \frac{N_T - R_T}{N_T + R_T}$$

And NIR_V is defined as

$$NIR_V = NDVI \cdot N_T$$

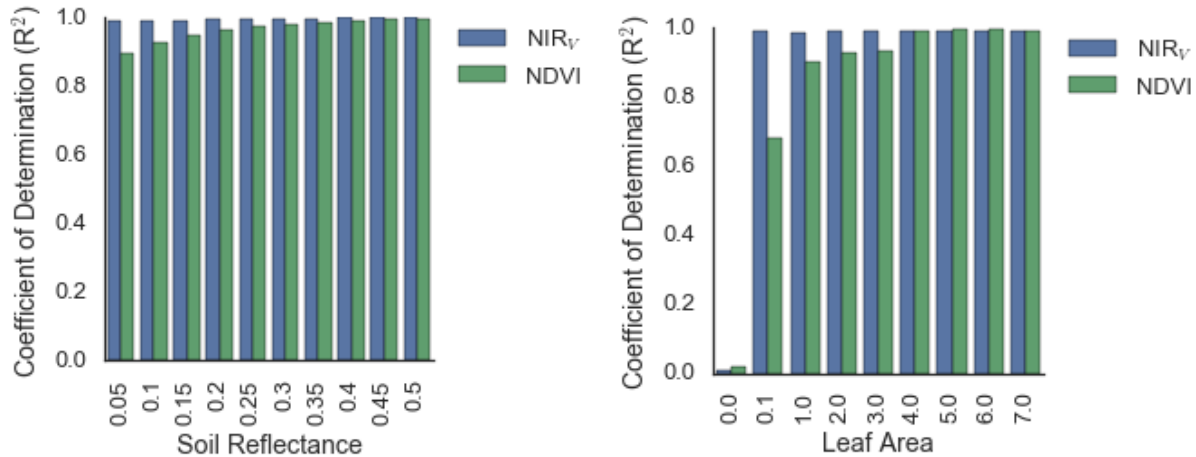


fig. S1. NIR_v more strongly predicts canopy fPAR than does NDVI. (A) Across all soil reflectance values and (B) across all leaf areas.

Across all model runs, NIR_v has a higher correlation with modeled fPAR than NDVI (fig. S1A). We can similarly show that NIR_v is better correlated to fPAR across all observed leaf-areas, where soil-reflectance is allowed to vary across the full range of modeled values (fig. S1B). More formally, NIR_v better normalizes for variations in LAI and soil reflectance than NDVI alone. Fig. S1 and S2, taken together, make it clear that variation in background reflectance drives the divergence in the two results. If we fit a regression through all available data, where both LAI and soil reflectance vary across their full ranges, the R^2 of the relationship between NIR_v and fPAR is higher than the R^2 between NDVI and fPAR. This requires that the variance in $\partial N_T \cdot NDVI / \partial \rho_s$ be less than the variance in $\partial NDVI / \partial \rho_s$. In the model, this difference matters most for low leaf-areas. Once leaf area exceeds 3, the differences between NIR_v and NDVI become trivial. In practice, the difference in approach results in a dramatic improvement in the ability to relate remotely sensed data to plant productivity.

text S2. 2D reflectance model

It is possible to demonstrate that the product of NDVI and total pixel reflectance (N_T) approximates the amount of NIR reflectance originating from vegetation (NIR_v) for any surface that is a mixture of soil and vegetation. We constructed a 2D pixel constituted of two classes: a

bare surface and a leaf. We specify a new parameter, f , that describes the fraction of the pixel covered by vegetation. The reflectance properties of both endmembers are fixed and take values according to table S2. For the non-vegetated fraction of the pixel, we assume that soil reflectance is constant across all wavelengths of the spectrum.

The total pixel reflectance of at any wavelength (λ) can then be calculated as the area-weighted sum of reflectance from vegetated and non-vegetated surfaces

$$\lambda_T = \lambda_V \cdot f + \lambda_S \cdot (1 - f) \quad (1)$$

where λ_V is the reflectance of the vegetated component of the pixel and λ_S is the reflectance of the soil component. Component-level NIR reflectances are specified with a N, while red reflectances are denoted with a R (e.g., table S2).

table S2. Model parameters used in 2D reflectance model. Vegetation reflectance values correspond to reflectance values of a semi-infinite canopy described in (9).

Medium	Red reflectance (R)	Near-infrared reflectance (N)
Soil	0.1	0.1
Vegetation	0.035	0.52

We are interested in exploring the relationship between NDVI and NIR_V and begin with the definition of NIR_V . For any configuration, NIR_V is defined as

$$NIR_V = N_V \cdot f \quad (2)$$

According to Equation 2, NIR_V represents the proportion of N_T that is reflected by and attributable to vegetation. It is important to distinguish what we are referring to as NIR_V from the actual NIR reflectance value of vegetation (N_V).

We continue with the definition of NDVI

$$NDVI = \frac{N_T - R_T}{N_T + R_T} \quad (3)$$

If we assume that soil reflectance is constant across all wavelengths ($N_S = R_S$), we can rewrite Equation 3 as follows

$$NDVI = \frac{N_V \cdot f - R_V \cdot f}{N_V \cdot f + R_V \cdot f + 2N_S \cdot (1-f)} \quad (4)$$

Under the condition that $R_V \ll N_V$, we can further reduce Equation 4 by eliminating the R_V terms

$$NDVI = \frac{N_V \cdot f}{N_V \cdot f + 2N_S \cdot (1-f)} \quad (5)$$

Using Equation 1, we can rewrite Equation 5 to read

$$NDVI = \frac{N_V \cdot f}{N_T + N_S \cdot (1-f)} \quad (6)$$

Finally, combining Equation 6 with Equation 2 yields

$$NIR_V = NDVI \cdot (N_T + N_S \cdot (1-f)) \quad (7)$$

Equation 7 makes it clear that under conditions where either $N_S \ll N_T$ or as f approaches 1, NIR_V equals the product of $NDVI$ and N_T .

This derivation relies on three simplifying assumptions. The first is that soil has constant reflectance, across all wavelengths. Second, R_V is significantly less than N_V . Finally, our derivation assumes that N_S is significantly less than N_T .

Even if we relax these three assumptions, the product of NDVI and N_T still serves as a useful proxy of NIR_V . We demonstrate this with a sensitivity analysis of Equation 1, where we vary f between 0 and 1, while randomly sampling parameter values from their full, empirically derived ranges (table S3). Sampling the full space shows that the product of NDVI and N_T closely approximates NIR_V (fig. S2; $R^2 = 0.99$; RMSE = 0.05). Furthermore, this calculated error likely represents an upper-bound, as many parameters within the model strongly covary (e.g, N_V and R_V), which constrains the realized parameter space.

table S3. Parameter ranges used in 2D reflectance model sensitivity test. N_V and R_V ranges taken from (39). N_V and R_V represent canopy-level reflectance values.

Parameter	Values
N_V	[0.3, 0.6]
R_V	(0, 0.05]
R_S	0.1, 0.3
N_S	$[R_S, R_S \cdot 1.2]$

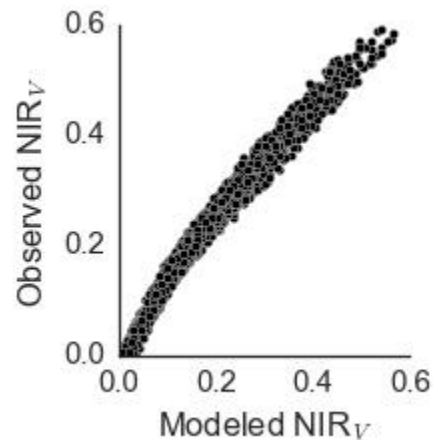


fig. S2. NIR_V as a function of NDVI and NIR_T . For each value of R_S , we independently selected 1,500 random combinations of the remaining model parameters outlined in table S3.

text S3. NIR_v and SIF simulations using SCOPE

The relationship between NIR_v and SIF is also found in radiative transport simulations, as demonstrated through a series of simulations using SCOPE v1.60. SCOPE is a one-dimensional, vertical energy balance and radiative transport model of the PROSPECT/SAIL family. SCOPE fully couples leaf biochemistry (including photochemical and non-photochemical processes) with chlorophyll fluorescence, making SCOPE useful for studying the biochemical and radiative transport processes that generate the SIF signal observed by satellite (37).

We ran thirty-six simulations where we varied leaf area, soil reflectance, canopy dry matter content, and fluorescence yield across runs, while holding other critical variables constant (table S2). We modified SCOPE to hold fluorescence yield constant to analyze the NIR_v-SIF relationship in purely structural terms. For each model run, we calculated SIF attributable to photosystem II at 740 nm and NIR_v from reflectances with nadir viewing geometry and a solar zenith angle of 30°. We calculated red reflectance using wavelengths between 640 nm and 670 nm and near-infrared reflectance from 850 nm to 870 nm. All simulations assumed a spherical leaf angle distribution.

table S4. SCOPE parameter values. We ran a total of 36 simulations, representing all combinations of leaf area, dry matter content, soil spectra, and fluorescence yield. *SCOPE includes multiple soil profiles, designated by number.

Parameter (Variable Name)	Units	Values
Leaf area index (LAI)	m ⁻² m ⁻²	1, 4, 7
Dry matter content (C _{dm})	g cm ⁻²	0.002, 0.005, 0.02
Chlorophyll a/b content (C _{ab})	μg cm ⁻²	50
Downwelling radiation (R _{in})	W m ⁻²	1500
Soil spectrum*	-	1, 3
Fluorescence yield (Φ _F)	-	0.01, 0.013

SIF and NIR_V have a strongly linear dependency, with NIR_V capturing 96 percent of the variation in SIF, when considering a single fluorescence yield (fig. S3). Changing fluorescence yield causes a linear offset between NIR_V and SIF. This offset indicates that NIR_V and SIF can be combined to further investigate the photochemical regulation of SIF, as NIR_V is a purely structural measurement.

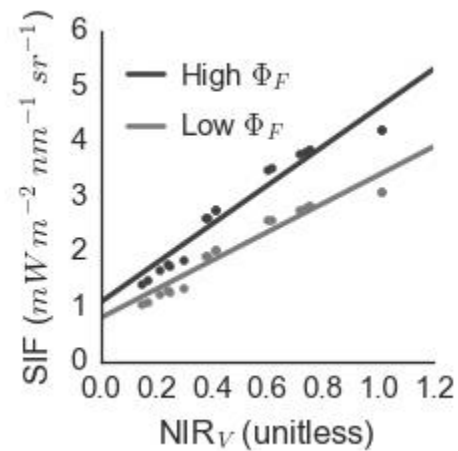


fig. S3. Linear relationship between modeled NIR_V and SIF. Data for both low (1 percent) and high (1.3 percent) fluorescence yields are shown. Disagreement between the SIF and NIR_V is highest for low leaf areas that have high canopy dry matter content.

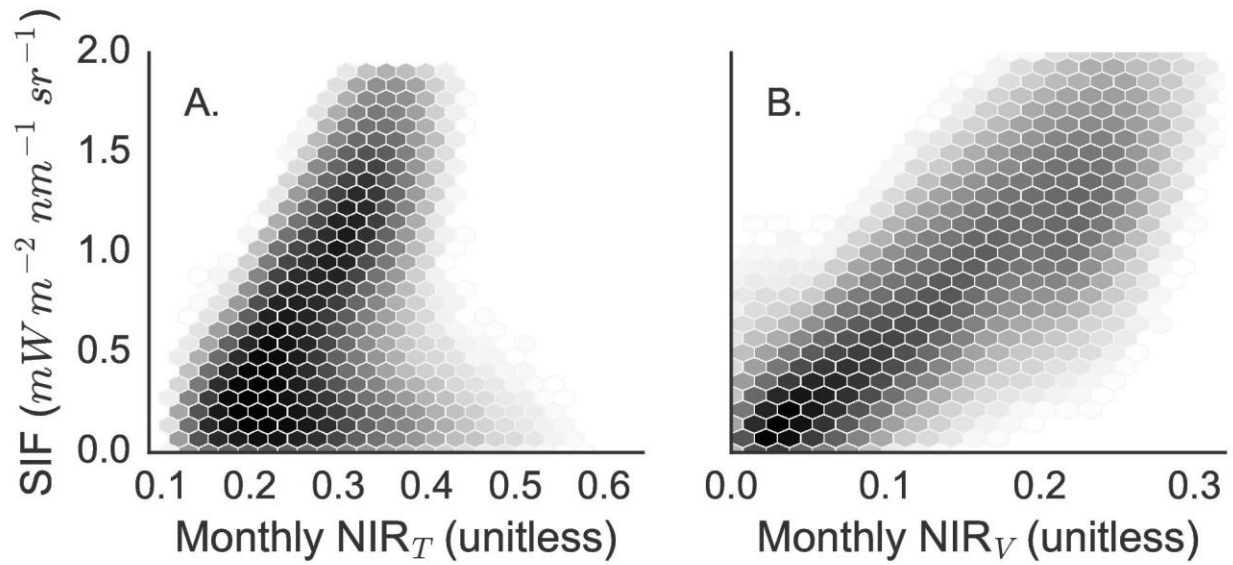


fig. S4. Comparison of the monthly MODIS-derived (A) NIR_T and (B) NIR_V against GOME-2 measurements of SIF. The ability of NIR_V to address the mixed pixel problem results from the combination of NIR with NDVI. NIR_T alone is a poor proxy of monthly SIF. MODIS estimates were aggregated to 0.5° from 500 meter scenes of BRDF-corrected reflectances. Shading indicates the logged number of pixels within each bin.

table S5. Multiyear monthly average NIR_v, fPAR, and GPP, by land cover classification for 105 FLUXNET sites. The difference in NIR_v at cropland and evergreen needleleaf sites is comparable to the difference in GPP, despite similar fPAR values. Data represent monthly values of NIR_v, fPAR, and GPP for the per-site month of maximum GPP.

Land Cover Class	NIR _v (unitless)	fPAR (unitless)	GPP (gC m ⁻² d ⁻¹)
Deciduous Broadleaf	0.28	0.72	11.18
Cropland	0.27	0.62	12.57
Mixed Forest	0.22	0.68	9.35
Grassland	0.19	0.55	6.61
Wetland	0.19	0.58	6.41
Evergreen Broadleaf	0.17	0.70	7.87
Evergreen Needleleaf	0.17	0.67	7.85
Savanna	0.15	0.45	5.62
Woody Savanna	0.14	0.42	6.23
Open Shrubland	0.13	0.48	3.85
Closed Shrubland	0.10	0.46	5.30